Drug Development and Industrial Pharmacy, 28(2), 177–191 (2002)

RESEARCH PAPER

A High-Throughput HERG Potassium Channel Function Assay: An Old Assay with a New Look

Charles S. Cheng,[1,†] Dawn Alderman,[2,†] Jennifer Kwash,[3] John Dessaint,[3] Rita Patel,[1] Mary Kay Lescoe,[1] Michele Bennett Kinrade,[1] and Weifeng Yu[2,*]

[1]*Department of Molecular Biology, Neurogen Corporation, 35 Northeast Industrial Rd, Branford, Connecticut 06405*
[2]*Department of High Throughput Pharmacology, Neurogen Corporation, 35 Northeast Industrial Rd, Branford, Connecticut 06405*
[3]*Department of Electrophysiology, Neurogen Corporation, 35 Northeast Industrial Rd, Branford, Connecticut 06405*

ABSTRACT

In this paper, we describe an assay using radioactive rubidium (^{86}Rb) efflux to screen functional human ether-a go-go-related gene (HERG) K^+ channels in a high-throughput screening (HTS) format. This assay offers an alternative way to examine functional interactions between chemical compounds and HERG K^+ channels. Follow-up experiments and discussions were carried out to address a variety of factors that affect potency evaluation within the Rb efflux assay. Factors that can affect the assay results, such as assay time, efflux rate, and compound blocking kinetics, are discussed in detail. Our results provide some explanations for the variances of the assay results and offer some guidelines for using the Rb efflux assay to evaluate compound interactions with HERG K^+ channels in the pharmaceutical industry.

Key Words: *Rubidium flux; High-Throughput Assay; HERG*

[†]These authors contributed equally.
*Corresponding author. Fax: (203) 483-8317; E-mail: wyu@nrgn.com

INTRODUCTION

Human ether-a go-go-related gene (HERG) was originally cloned from human hippocampus by Warmke and Ganetzky (1) and is strongly expressed in the heart (2). Molecular, genetic, and physiological function studies suggest that HERG encodes the pore-forming subunit of cardiac I_{kr} potassium (K^+) channels (2–4). Its inheritance in mutant form is associated with long QT syndrome (LQTS), a disorder that predisposes one to torsades de pointes and ventricular fibrillation (2,3,5). HERG is also a target for blockade by many drugs, including some noncardiovascular therapeutic agents (4,6–9). Blockade of HERG K^+ channels causes prolongation of cardiac repolarization or the QT interval in the electrocardiogram (ECG), which can lead to the generation of the life threatening ventricular arrhythmia known as torsades de pointes (10–12). In 1997, the European Agency for Evaluation of Medicinal Products of the Committee for Proprietary Medicinal Products (CPMP) issued new guidelines (13) concerning studies to be carried out to assess the risks incurred with noncardiovascular therapeutic agents for cardiac function; in particular, evaluation of prolongation of the QT interval in ECG. This document caused considerable concern within the pharmaceutical industry and prompted development of assays to evaluate this cardiovascular risk.

Electrophysiology assays, specifically whole-cell voltage clamp, have been used to study a variety of receptors and ion channels, including HERG K^+ channels (4,6,14–17). Because of its high resolution, an electrophysiology assay is well suited to study the multiple properties of HERG K^+ channels, including drug effects on the channel. These studies can provide accurate information about the biophysical properties of HERG K^+ channels and accurate potency estimates for HERG blocking drugs. However, the major drawback of the electrophysiology assay is slow throughput. Given current techniques, it is difficult to assess hundreds of compounds in a short period of time. With increasing numbers of potential drugs in development and increasing concerns for drug safety, the need for a high-throughput screening (HTS) assay of HERG K^+ channels is increasing. Radioactive dofetilide binding has been used to study the HERG K^+ channels (18–20). This assay provides a biochemical view of compound interaction with the established dofetilide binding site within HERG K^+ channels. It also provides a foundation for HERG HTS assay. However, dofetilide binding on wild-type HEK 293 cells was reported (21), which could affect the binding data interpretation. Discrepancies between HTS and electrophysiology assay results have been seen in a dofetilide binding study (20). The availability of dofetilide and its patent issues also limit its usage from a broader pharmaceutical industry. Therefore, efforts to develop HTS assays for HERG K^+ channels have continued.

Radioactive rubidium (^{86}Rb), which is easily obtained and relatively inexpensive, has been used as a tracer to study K^+ channels (22–25) and Na^+ channels (26–28). In this paper, we describe an assay using Rb efflux to screen functional HERG K^+ channels in a HTS format. This assay offers an alternative way to examine functional interactions between chemical compounds and HERG K^+ channels in a HTS format. However, the assay does not provide the sensitivity that an electrophysiology assay does. Follow-up experiments and discussions were carried out to address the differences observed between Rb efflux and electrophysiology assays. Factors that can affect the efflux assay results, such as assay time, efflux rate, and compound blocking kinetics, are discussed in detail. Our results provide some explanations for the differences observed between Rb efflux and electrophysiology assays. Based on our data, we offer some guidelines for using Rb efflux assay to evaluate compound interactions with HERG K^+ channels in the pharmaceutical industry.

MATERIALS AND METHODS

Cloning of the HERG Gene

In order to screen cDNA libraries for the HERG gene, probes were generated using the following primer pairs derived from the published sequence for the HERG gene (Genebank accession # HSU04270). (1) Forward primer: 5′GCTTCCTATG TCTGGTGGATGTG, reverse primer: 5′TGTGGG TTCGCTCCTTTATCTTAG. (2) Forward primer: 5′CCATCAAGGACAAGTATGTGACGG, reverse primer: 5′TACAGGTTCAGAGGCTCCCCAAAG. Oligonucleotide primers used for cloning were synthesized by the W.M. Keck Biotechnology Resource Laboratory at Yale University on an ABI 392 DNA synthesizer. Screening of a human

heart cDNA library (Stratagene, La Jolla, CA, catalog # 937257) yielded a full-length HERG cDNA sequence. The HERG cDNA was then sub-clone into the pIRES vector (Clontech, Palo Alto, CA, catalog # 6064-1) and the HERG sequence was verified according to the published information.

Transfection and Maintenance of CHO Cell Line

The pIRES vector plasmid containing the HERG gene was used to transfect Chinese hamster ovary (CHO) cells (CHO-K1 from ATCC, Manassas, VA). The transfection was performed with a Lipofectamine Plus Transfection kit from Gibco BRL (Grand Island, NY, catalog # 10964-013). The manufacturer's protocol was followed with the following exception: 8 μg of DNA plasmid was used for a 10-cm plate, which was seeded with 1.5×10^6 cells/plate overnight prior to transfection. A stable pool of cells was selected by incubating the transfected cells for two weeks in the CHO-K1 selection media [Ham's F-12 1× (Mod.) with L-glutamine (catalog # 10-080-CM from Cellgro Company, Herndon, VA) to which was added 10% fetal bovine calf serum (JRH, Lexna, KS, catalog # 12106-78P) and 400 μg/mL G418 (Genticin brand from Sigma, St. Louis, MO, catalog # G-9516) and 25 mM HEPES buffer]. From this stable pool of cells, one cell per well was seeded into a few 96-well plates (Costar 96-well cluster plate 3904, Corning Industries, Corning, NY). Cells plated in this manner were also grown under the same selection media detailed above. Individual colonies were then picked and assayed for HERG activity by Rb efflux and electrophysiological recordings. The cells permanently expressing HERG K^+ channels were maintained by being passed twice per week. Cells were maintained at 37°C and 5% CO_2 throughout the selection process.

Rubidium (Rb) Efflux Assay

Cells were seeded into 96-well plates (Falcon 35-3075, Becton Dickinson, Boston, MA). Cell density was 200 cells/μL of media [Ham's F-12 1× (Mod.) with L-glutamine (catalog # 10-080-CM from Cellgro Company)] and 150 μL of this cell-containing media was used to seed each well. After seeding, the cells were incubated at 37°C and 5% CO_2 overnight prior to use. For the Rb efflux assay, the cell culture medium was changed to rubidium (^{86}Rb) (Dupont NEN, Boston, MA) containing (1 μCi/mL of media), with 100 μL for each well of the 96-well plate. The cells were incubated in the Rb-containing media for 4 hr at 37°C and 5% CO_2. After Rb loading, the excess Rb-containing media was aspirated off using a Sigma multiwell platewasher/dispenser manifold (Sigma M-2531). Cells were then washed five times with 100 μL of the washing buffer. The washing buffer contains: 140 mM NaCl, 2 mM $CaCl_2$, 5 mM KCl, 2 mM $MgCl_2$, 10 mM HEPES, and 10 mM glucose. The pH was adjusted to 7.4 with NaOH (all reagents obtained from Sigma). The high K^+ test buffer was then transferred into the wells immediately after the wash cycles had been completed. The 65 mM K^+ test buffer contains: 80 mM NaCl, 2 mM $CaCl_2$, 65 mM KCl, 2 mM $MgCl_2$, 10 mM HEPES, and 10 mM glucose. The pH was adjusted to 7.4 with NaOH (all reagents obtained from Sigma). The 40 mM K^+ test buffer contains: 105 mM NaCl, 2 mM $CaCl_2$, 40 mM KCl, 2 mM $MgCl_2$, 10 mM HEPES, and 10 mM glucose. The pH wes adjusted to 7.4 with NaOH (all reagents obtained from Sigma). The test compounds were carried in the high K^+ test buffer. After incubation at room temperature for the specific time duration of the experiment, the high K^+ test buffer was then extracted from each well and transferred into a corresponding well in a Wallac 96-well Flexplate (Wallac 1450-401, Wallac Oy, Turku, Finland). This plate was then sealed with a Wallac resealable tape sheet (Wallac 1450-462) and counted as the efflux plate. One hundred microliters of 0.1% SDS solution was then transferred into each of the extracted cell plate wells to lyse the cells. After a 10-min incubation, the SDS solution was extracted from each well and transferred into a corresponding well in another Wallac 96-well plate. This plate was sealed and counted as the residual plate. These Wallac plates were read in a counter (Wallac Trilux 1450 MicroBeta Liquid Scintillation and Luminescence counter, 12 Detector Model). The digital data generated by the counter were analyzed with Microsoft Excel and Origin software. The result is expressed as a percentage of efflux, calculated as follows:

$$\% \text{ efflux} = \text{flux plate}/(\text{flux plate} + \text{residual plate})$$

Test compounds were obtained as follows. E-4031 was purchased from Biomol (Plymouth Meeting, PA). Astemizole was purchased from Sigma (St. Louis, MO). Dofetilide was a gift from Pfizer Inc. (Groton, CT).

Electrophysiology Recordings

Standard whole-cell recording (29) was carried out on the CHO cells permanently expressing HERG K^+ channels as previously described. Microelectrodes were pulled from 1.5-mm glass (World Precision Instruments, TW100-4) on a horizontal puller (Sutter Instrument Company, Model P-87). Electrodes had resistances between 2 and 3 MΩ when filled with internal solution. The internal solution contains: 100 mM KF, 40 mM KCl, 5 mM NaCl, 10 mM EGTA, and 10 mM HEPES, adjusted to pH 7.4 with KOH. The cells were perfused with external solution containing: 140 mM NaCl, 2 mM $CaCl_2$, 5 mM KCl, 2 mM $MgCl_2$, 10 mM glucose, and 10 mM HEPES, adjusted to pH 7.4 with NaOH. The junction potential calculated using pClamp 8 software was −7.4 mV (Axon Instruments) and corrected accordingly. Currents were filtered at 5 kHz on an Axopatch-1D amplifier (Axon Instruments) and recorded onto a PC with sample rate of 1 kHz using pClamp 8 (Axon Instruments). Data were analyzed using Clampfit (Axon Instruments) and Origin software (Microcal). Stock solutions for compounds were made in dimethylsulfoxide (DMSO) at a concentration of 10 mM. The final test concentration was achieved by diluting the stock solution directly into the external solution.

RESULTS AND DISCUSSION

A CHO cell line stably expressing HERG K^+ channels was established (see Materials and Methods). Whole-cell voltage clamp recordings were carried out on the cells. Figure 1 shows representative whole-cell currents for a series of voltage steps

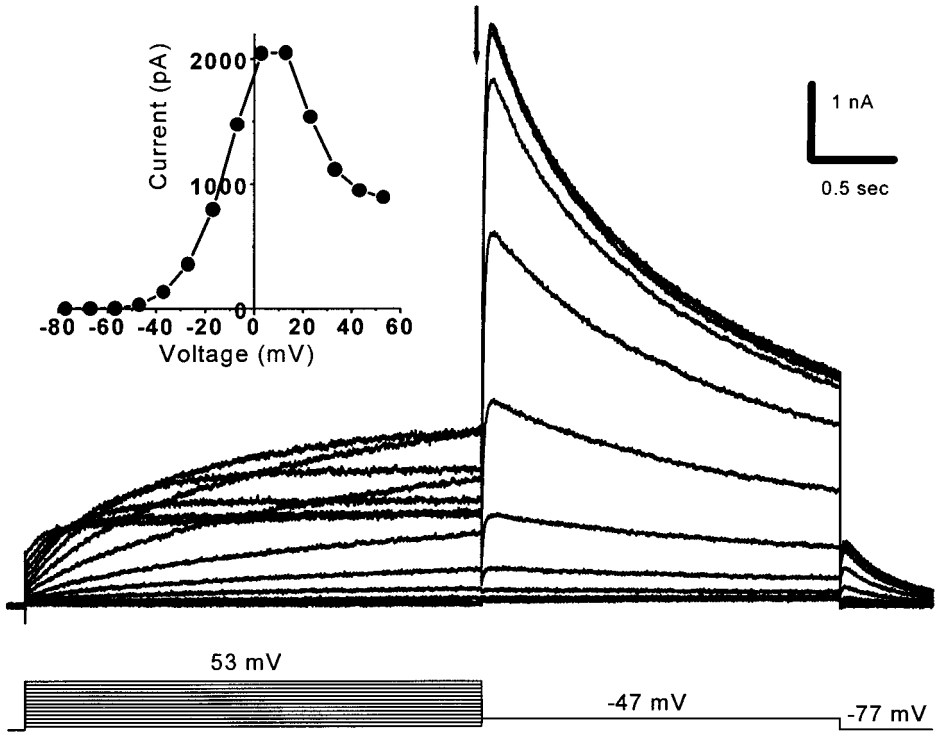

Figure 1. Whole-cell electrophysiology recording from CHO cells permanently expressing HERG K^+ channels. The membrane potential was held at −77 mV and stepped to a series of testing voltage from −67 to 53 mV in 10 mV increments as indicated by the bottom traces. The currents evoked were illustrated with tail current obtained at a voltage of −47 mV. The insert illustrates the *I–V* curve taken from the same cell. The current was taken at the time indicated by the arrow.

recorded from a HERG expressing cell. The membrane potential was held at −77 mV and stepped up to 53 mV in 10 mV increments. The tail current was obtained when the testing voltage was stepped down to −47 mV. A characteristic HERG K^+ current was observed with inward rectification shown at positive potentials (see the insert to Fig. 1), which is consistent with the reported properties of HERG K^+ currents (3,6,30). The current is also sensitive to specific HERG K^+ channel blocker, E-4031 (see Fig. 6C later) (30–33). These results confirmed that the cell line in our study was stably expressing HERG K^+ channels. This cell line was used for the rest of the Rb efflux studies.

For Rb efflux studies, the opening of HERG K^+ channels was achieved by increasing extracellular K^+ concentration to 65 mM, which depolarizes the cell membrane due to the K^+ reversal potential change. A time-dependent Rb efflux can be measured in a 96-well/plate format, as illustrated in Fig. 2A. The time-dependent Rb efflux was clearly seen after high K^+ application, and this increase was sensitive to specific HERG channel blocker, E-4031. The largest difference is Rb efflux between activation and blockade of the channels was obtained within a time window between 25 and 45 min. This time window provided the best signal-to-noise ratio and was chosen for conducting the Rb efflux assay. Different HERG antagonists, dofetilide (6,17,34), astemizole (9,35), and E-4031, were tested. As shown in Fig. 2B, the HERG antagonists eliminated the Rb efflux induced by high K^+ application, suggesting that the efflux increase is through HERG K^+ channels. Slightly lower than control Rb efflux was observed under high concentration of HERG blocker (10 μM astemizole). This may indicate the possibility of efflux leak through HERG channels under the control condition. Zhou et al. (31) reported that the resting membrane potential was shifted to the hyperpolarization direction after HERG K^+ channels were expressed in HEK 293 cells, suggesting that there was some level of HERG channel activation at rest. Our results, that lower than control efflux was observed under high concentration of HERG blockers, are consistent with this interpretation. Overall, our results provide a basic format for HTS HERG K^+ channels.

For industrial HTS, assay consistency is a crucial requirement. We monitored the assay consistency by monitoring its efflux rate and data reproducibility. Figure 3A shows three time courses of Rb efflux

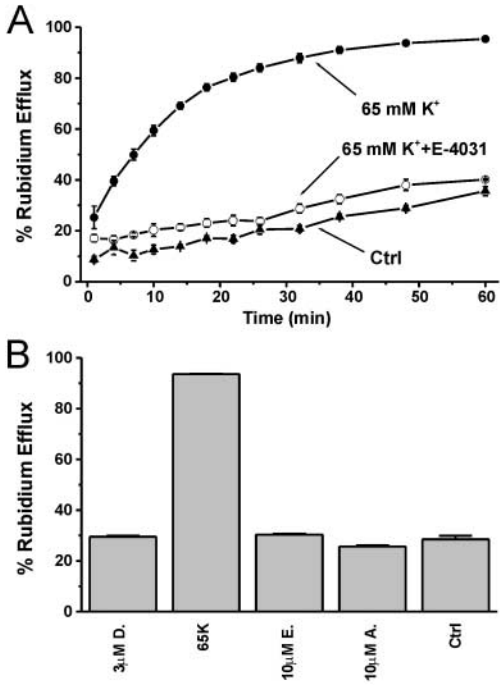

Figure 2. Specific HERG K^+ channel blockers inhibit Rb efflux. The experiments were carried out in a 96-well/plate The Rb efflux was evoked by 65 mM extracellular K^+. The efflux was taken from a set of wells at a given time and was calculated for that time. (A) The averaged result from three independent experiments was plotted. The 65 mM K^+ evoked a time-dependent Rb efflux that was significantly reduced by E-4031 (10 μM), a specific HERG K^+ channel blocker. The efflux leak was measured without extracellular high K^+ and shown as control. (B) Comparison of several known HERG channel blockers shows a consistent reduction of Rb efflux down to the basal control level. Data shown were taken after 40 min incubation with test compounds and high K^+ (65 mM) activation buffer. The bars represent the mean values of the percentage Rb efflux averaged from 16 wells for each condition. The error bars indicate the Standard Error of the Mean SEM. Compound abbreviations: D = dofetilide, E = E-4031, A = astemizole, Ctrl = low K^+ buffer (see Materials and Methods).

done independently is three different weeks. The observed efflux rate was stable, suggesting that HERG expression was stably maintained during this experimental period. Our later experiments provided evidence that the HERG expression could be stably maintained for several months (data not shown). The stable HERG expression and efflux rate indicate that the Rb HERG assay is consistent and robust. The assay consistency was

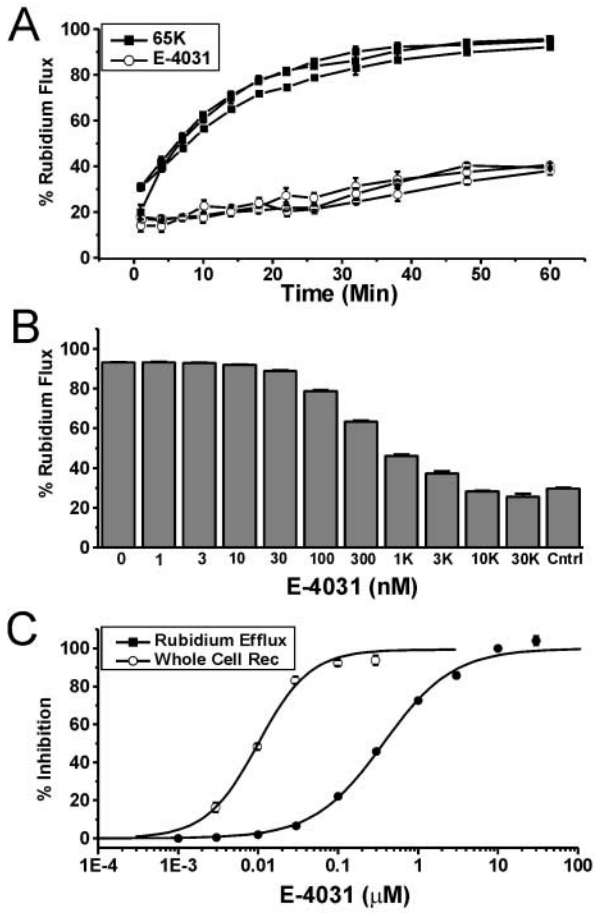

Figure 3. Dose-dependent inhibition of Rb efflux by HERG antagonist E-4031. (A) A time course of Rb efflux was run. The evoked efflux was achieved by 65 mM extracellular K^+ application. E-4031 (10 μM) significantly reduced the efflux rate. For each data point, efflux was averaged from three to five wells and the mean was expressed. The error bars represent SEM. Three independent time courses of Rb efflux are shown. The maximum signal-to-noise ratio was achieved with 40 min of incubation. Therefore, subsequent data (shown in B) was collected at this time point. (B) Rb efflux was done under different concentrations of E-4031 (from 1 nM to 30 μM). Each bar graph represents the averaged percentage efflux from 12 wells. The error bars represent the SEM. (C) Dose–response curves were plotted for E-4031 with electrophysiology assay (open circles) and Rb efflux assay (filled circles). For the Rb efflux assay, data were taken from (B) and normalized according to 10 μM E-4031. The solid lines represent the fitted curves when both sets of data were fitted with a logistic equat nM (10.2 ± 0.2 nM) with Hill coefficient of 1.3 (1.3 ± 0.1). For the Rb efflux assay, the IC_{50} was 368 nM (368 ± 25 nM) with Hill coefficient of 1.0 (1.0 ± 0.1).

further tested through our compound screenings (see discussion below). The next question we posted was whether the reduction of Rb efflux by antagonists (as shown in Fig. 2B) is dose-dependent. Figure 3B shows raw data on the dose-dependent blockade of Rb efflux by E-4031 when assayed at 40 min. Increasing the concentration of E-4031 increases its blockade on the Rb efflux. When data were normalized according to the blockade of 10 μM E-4031, a dose–response curve was plotted (Fig. 3C, filled square). An IC_{50} of 349.4 nM and a Hill coefficient of 1.0 were obtained when the data were fitted with the logistic equation (% inhibition $= 100/\{1 + [(IC_{50})/(\text{Conc.})]^n\}$) (Fig. 3C, solid line). However, when this IC_{50} was compared with the IC_{50} obtained through a whole-cell voltage clamp (Fig. 3C, open circle), a significant potency shift was apparent. An IC_{50} of 10.2 nM with a Hill coefficient of 1.3 was obtained for E-4031 through a voltage clamp (Fig. 3C, open circle). This electrophysiology result is consistent with published data (30,31), which showed IC_{50} values for E-4031 from 7.7 to 134 nM. Therefore, the potency difference between these two assays seems to be assay-related. Similar dose–response curves were also carried out for dofetilide (Fig. 4A) and astemizole (Fig. 4B). The normalized dose–response curves are shown in the insert and fitted with a logistic equation. The IC_{50} is 84.1 ± 4.8 nM with Hill coefficient of 1.2 for dofetilide and 0.36 ± 0.02 μM with Hill coefficient of 1.6 for astemizole. These values are also shifted to the right from published IC_{50} values obtained through electrophysiology assay: 12 nM for dofetilide (6), 0.9 nM for astemizole (35), and 4.2 nM for astemizole from our own data (not shown). Once again, the potency difference between electrophysiology and Rb efflux assays is shown. We conducted the following experiments to address some of the reasons underlying this difference. Our studies provided some explanations for this assay-related difference and practical guidelines for using HTS Rb efflux assay in the pharmaceutical industry.

Rb efflux through the HERG K^+ channels can be fitted with a single exponential curve. In order to illustrate the time-dependent Rb efflux, the efflux data shown in Fig. 2A were modified as follows. The baseline Rb efflux taken at 1 min in control was subtracted from the stimulated efflux. The subtracted efflux was then normalized according to the maximum efflux assigned at 60 min. The modified data are plotted in Fig. 5A (filled circles),

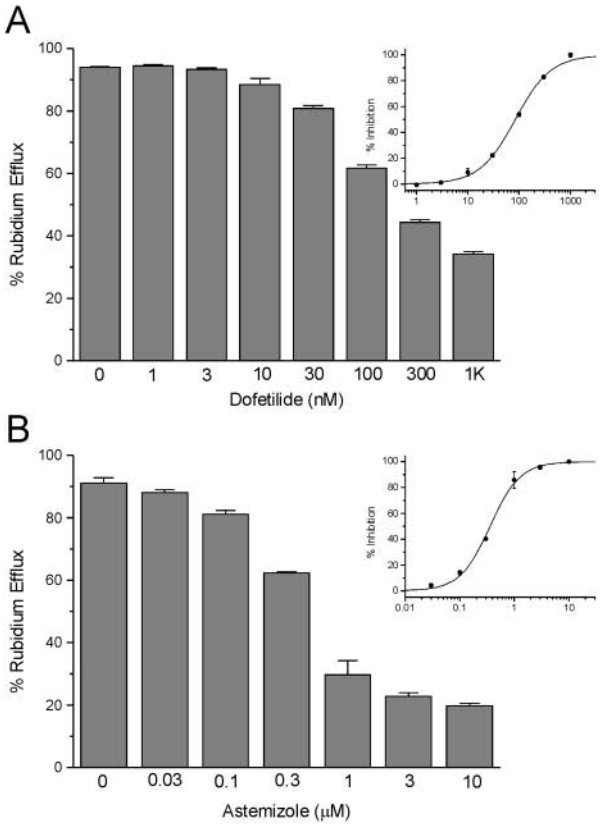

Figure 4. Dose-dependent inhibition of Rb efflux by HERG antagonists, dofetilide, and astemizole. Rb efflux assay was done for different concentrations of dofetilide (from 1 nM to 1 μM): (A) with assay time of 40 min and astemizole (from 30 nM to 10 μM) and (B) with assay time of 30 min. Each bar graph represents the averaged percentage efflux from six wells. The error bar represents the SEM. The insert shows the normalized dose–response curve and the logistic fitted curve. The IC_{50} was 84.1 nM (84.1 ± 4.8 nM) with Hill coefficient of 1.2 (1.2 ± 0.1) for dofetilide and 360 nM (360 ± 20 nM) with Hill coefficient of 1.6 (1.6 ± 0.1) for astemizole.

fitted with a single exponential equation [$Y = 100(1-e^{(-t/\tau)})$] with a time constant of 12.53 min, as shown by the solid line. If we assume that blocking HERG K^+ current in a whole-cell voltage clamp reflects the reduction of channel open probability, the Rb efflux under a HERG blocking agent will adopt a new time constant (τ) that can be calculated as follows:

$$\tau_{new} = \tau_{control}/(1 - \%\ \text{inhibition})$$

Here τ_{new} represents the new time constant, $\tau_{control}$ represents the time constant without antagonists, and % inhibition represents the percentage inhibition obtained under voltage clamp condition. For example, if compound A at a fixed concentration blocks HERG current by 50% in electrophysiology assay, the new time constant under compound A at the same concentration will be twice as long as the control. A 100% inhibition in electrophysiology assay will mean a theoretical time constant of infinity in Rb efflux assay. Figure 5A shows theoretical efflux curves when 30%, 50%, 70%, 90%, and 99.99% of current is blocked in a voltage clamp. If we use 99.99% inhibition curve as the negative control and the stimulated curve as the positive control for our Rb efflux assay, the rest of the Rb efflux data can be normalized accordingly. For example, if we set up our assay time at 40 min, a compound that shows 50% inhibition in electrophysiology only registers a 17% reduction in Rb efflux (open circle in Fig. 5A). This example illustrates that percentage inhibition for any given compound will be different depending on the assays employed, with a higher percentage inhibition being observed in electrophysiology than in Rb efflux assay.

Another striking difference observed is how the percentage inhibition in Rb efflux assay can be significantly affected by the length of assay time. As illustrated in Fig. 5A, a high signal-to-noise ratio is obtained when the assay is carried out at the 40-min time point. At this time point, however, the ability to read the accurate biophysical inhibition for a compound is reduced. For example, following the same 50% inhibition curve as shown in Fig. 5A, about 46.6% inhibition will be obtained at 4-min assay time point for the same compound that shows only 17% inhibition at the 40-min assay time point (open circle in Fig. 5A). Evidently, a higher potency value for a compound is obtained when the assay time is shorter. To further discuss the effect of assay time on the evaluation of potency, a model compound is assumed. We assume an ideal compound with 1 nM IC_{50} and a Hill coefficient of 1 in electrophysiology for blocking HERG K^+ channels. Using the Rb efflux rate generated from our experiments (solid fitting curve in Fig. 5A), we can model the percentage inhibition at any given time in the Rb assay. Figure 5B shows dose–response curves generated by the model at assay times of 40 min (filled circles) and 4 min (open circles). When assay time is set at 40 min, Rb efflux assay generates

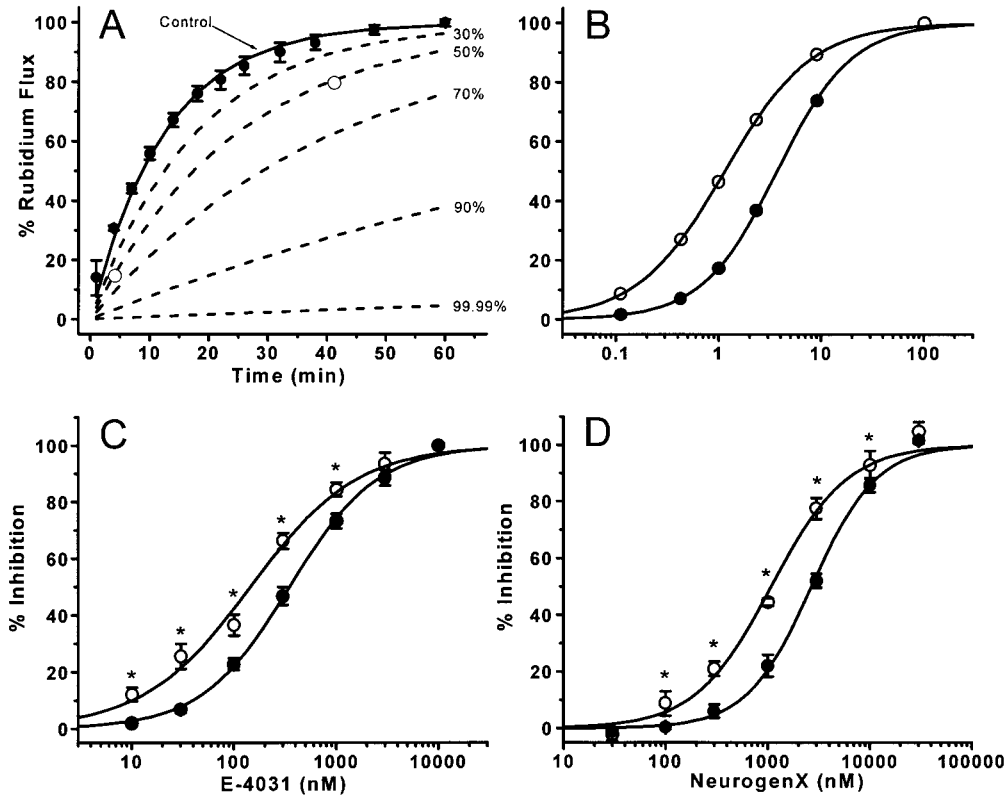

Figure 5. Assay time significantly affects the compound potency evaluation in Rb efflux assay. (A) The same data shown in Fig. 2A were leak subtracted and normalized according to the efflux at time 60 min. Data were then fitted with a single exponential [$Y = 100(1 - e^{(-t/\tau)})$] with a time constant ($\tau$) of 12.53 min (12.53 ± 0.37 min) (solid line). A new value τ_{new} could be calculated according to the equation [$\tau_{new} = \tau_{control}/(1 - \text{inhibition})$], where $\tau_{control}$ is 12.53 min. When the inhibition was 30%, 50%, 70%, 90%, and 99.99%, the calculated efflux traces [$Y = 100(1 - e^{(-t/\tau)})$] are plotted as the dashed lines with percentage inhibition shown on the right-hand side. Two open circles indicate the calculated % Rb efflux at time 4 and 40 min when 50% inhibition is achieved electrophysiologically. (B) Dose–response curves are calculated at time 4 min (open circle) and 40 min (filled circle) for an assumed compound which has an IC_{50} of 1 nM and Hill coefficient constant of 1 in electrophysiology assay. The calculation was done based on the efflux equation $Y = 100(1 - e^{(-t/\tau)})$ and time constant τ [$\tau_{new} = \tau_{control}/(1 - \text{inhibition})$] calculation. The calculated efflux was then normalized according to the blockade achieved by a 100 nM concentration that has an assumed 99% inhibition in electrophysiology assay. When fitted with a logistic equation for both curves, an IC_{50} of 1.14 nM with Hill coefficient of 1.0 is obtained for the 4-min assay and an IC_{50} of 3.68 nM with Hill coefficient of 1.2 for the 40-min assay. About a 3-fold shift in compound potency is generated by the different assay times in this model run. (C, D) Dose–response curves were obtained for E-4031 (C) and a Neurogen internal HERG antagonist, NeurogenX (D) at 4-min assay (open circle) and 40-min assay (filled circle). Data represent the average from three to five independent experiments for both compounds. The error bars in both graphs indicate the SEM. For both compounds, the potency was shifted (about 2.5-fold) by switching the assay time from 4 min to 40 min. Asterisks indicate significant difference at the 0.05 levels.

an IC_{50} of 3.68 nM with a Hill coefficient of 1.2 for our model compound. On the other hand, an IC_{50} of 1.14 nM with a Hill coefficient of 1.0 is obtained if the assay time is carried out at 4 min. An approximately 3-fold potency shift is generated by the two assay times.

In order to validate our model, we ran Rb efflux assays for two HERG channel blockers at different assay times. As shown in Fig. 5C, when assayed at the 4-min time point, an IC_{50} of 140 nM with a Hill coefficient of 0.8 was obtained for E-4031 (open circle). However, when the assay time was moved

to the 40-min time point, an IC_{50} of 350 nM with a Hill coefficient of 1.0 was obtained (filled circle). An approximately 2.4-fold potency shift was observed. Figure 5D shows the Rb efflux assay results of an internal HERG K^+ channel antagonist, NeurogenX. An IC_{50} of 1.1 μM with a Hill coefficient of 1.2 was obtained when the assay was done at 4 min (open circle). An IC_{50} of 2.7 μM with a Hill coefficient of 1.4 was obtained when assayed at 40 min (filled circle). About a 2.5-fold potency shift was observed for this compound. For both compounds, E-4031 and NeurogenX, a significant IC_{50} shift was produced when assayed at two different time points. This shift is close to the value predicted by our model, where an approximately 3-fold potency shift is expected. These experiments and our model showed that the evaluation of compound potency on HERG K^+ channels using Rb efflux assay critically depends on the assay time. A significant potency shift can be generated by different assay times.

As discussed above, the evaluation of potency could be affected by the assay time. However, at any given assay time, the rate of Rb efflux should also affect the potency evaluation. It is possible to conceive that a compound with 50% inhibition in electrophysiology may not show detectable inhibition in Rb efflux assay if the control has an efflux time constant less than 1 min and the assay is carried out at the 40-min time point. To modify the rate of efflux to test its impact on potency, we modified the membrane potential by using different extracellular K^+ concentrations. As a voltage-gated K^+ channel (2–4), the open probability of the HERG K^+ channel critically depends on the membrane potential. Lowering the extracellular K^+ concentration from 65 to 40 mM lowers the effective membrane potential as calculated by the Nernst equation, which in turn decreases the open probability of HERG K^+ channels. Since the HERG channel conductance is also sensitive to extracellular K^+ concentration (3,36), lowering extracellular K^+ concentration also decreases the channel conductance. The net effect of this change results in a slower rate of Rb efflux, as illustrated in Fig. 6A. The rate of Rb efflux was slower with 40 mM extracellular K^+ (filled circles) than with 65 mM K^+ (filled squares). With a reduced Rb efflux rate, higher potency for a given HERG antagonist was expected when compared with that at a higher efflux rate. Figure 6B illustrates the effect of reduced efflux rate on the apparent potency of E-4031. The dose–response curve was obtained at the assay time of 10 min with 40 mM extracellular K^+ (open circles), since the signal-to-noise ratio was too small to get an accurate reading at the 4-min time point. When fitted with the logistic equation, an IC_{50} of 79.2 nM with a Hill coefficient of 1.1 was obtained for E-4031. The result was then compared with that obtained at 4 min with 65 mM extracellular K^+ (filled circle in Fig. 6B). A 1.8-fold leftward shift was observed. As previously discussed, assay at a later time point tends to shift the potency to the less potent direction. If we could assay at the 4-min time point with 40 mM K, the potency shift would be even higher than the 1.8-fold observed. So far, our model and experimental data suggest that the potency evaluation in Rb efflux assay can be affected by at least two factors: assay time and Rb efflux rate. With these factors in mind, caution should be taken when experimental results obtained in Rb efflux assay are compared with the data from electrophysiology.

The IC_{50} of 79 nM for E-4031 estimated with Rb efflux (see Fig. 6B) is still less potent than that obtained from electrophysiology, which is 10.2 nM (see Fig. 3C, open circles). Modifying the Rb efflux assay conditions, such as lowering the rate of efflux further as demonstrated above, may further improve the accuracy of the reading. However, other factors can also affect the results in the Rb efflux assay. One of these additional factors is discussed below. Many K^+ channel antagonists show the characteristics of open channel blockers, such as E-4031 and dofetilide for HERG K^+ channels (6,32). Channel activity is needed in order for the antagonist to block the channel. However, channel opening in Rb efflux assay initiates the Rb efflux. Time delay of blocking activity will eventually affect the final Rb counts at the assay point, i.e., the reduction of the Rb efflux by the antagonist. Figure 6C shows the time course of 100 nM E-4031 blocking HERG K^+ current in a whole-cell voltage clamp recording. E-4031 was applied to the cell at the time indicated by the first arrow. The peak tail current vs. time was plotted. A gradual reduction of the HERG K^+ current was observed with E-4031 application. A final 97% inhibition was observed after about 10 min of E-4031 application. Traces taken at the arrow points are shown in the insert. Even though the perfusion is different when compared with the incubation condition in Rb efflux

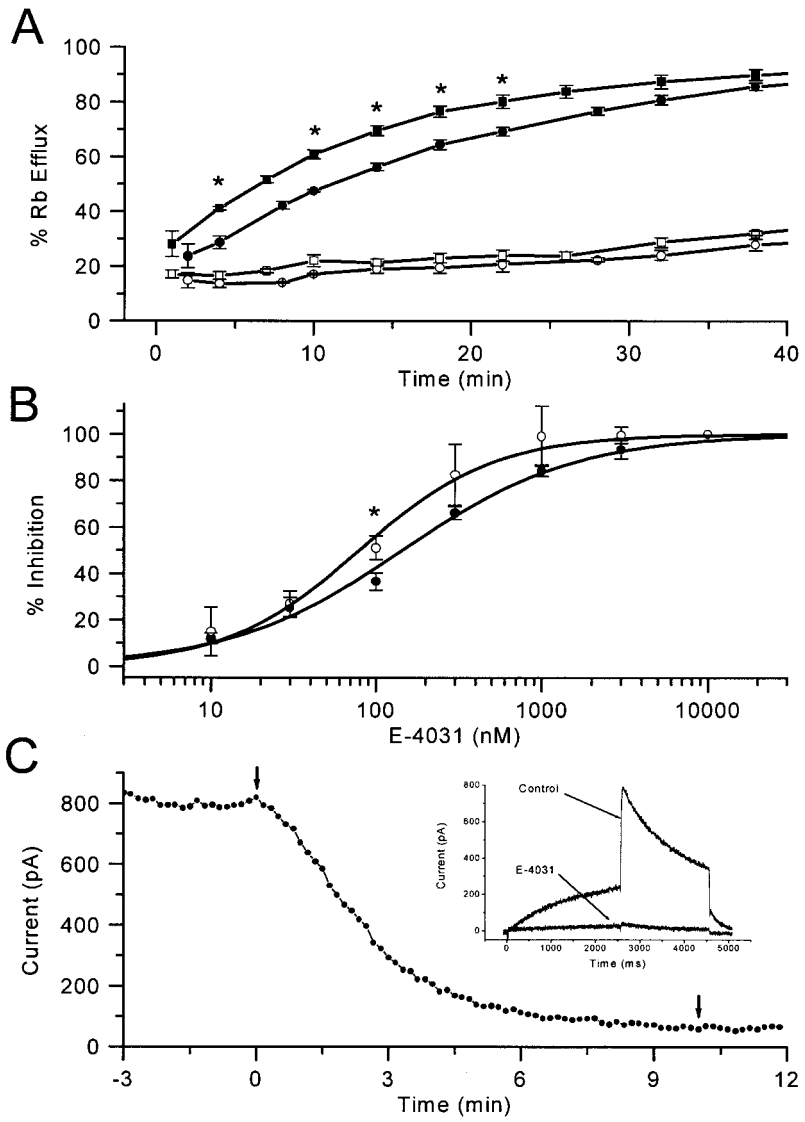

Figure 6. The rate of efflux and compound blocking kinetics can also affect the potency evaluation in Rb efflux assay. (A) Using a 40 mM extracellular K^+ solution to activate the HERG channel produces a slower rate of Rb efflux compared with using a 65 mM extracellular K^+ solution. The squares represent Rb efflux using 65 mM K^+ with (open square) and without (filled square) 10 μM E-4031. The circles represent Rb efflux done using 40 mM K^+ with (open circle) and without (filled circle) 10 μM E-4031. Data represent the average from three independent experiments. The error bars represent SEM. Asterisks indicate significant difference at 0.05 level. (B) Dose–response curves for E-4031 were generated in a 10-min assay using 40 mM K (open circles) and a 4-min assay using 65 mM K (filled circles). Data were averaged from three independent experiments. The error bars represent SEM. Asterisks indicate significant difference at 0.05 level. Slowing the rate of the Rb efflux shifted the E-4031 dose–response curve to the left, providing a higher observed potency. (C) Whole-cell recording illustrates the prolonged time needed to observe the maximum effect of E-4031. Whole-cell recording was carried out on a CHO cell permanently expressing HERG channels. The membrane potential was held at −77 mV and a depolarizing voltage pulse to 3 mV was delivered to open the HERG channels for 2.5 sec. The tail current was monitored at a voltage of −47 mV for 2 sec. This pulse protocol was applied every 10 sec and the peak tail current was plotted vs. time. The drug is directly superfused onto the cell beginning at time zero. Maximum effect for the drug is not observed until ~10 min after the start of superfusion. The insert illustrates the control and blocked HERG currents taken at the points indicated by arrows.

assay, the figure still illustrates that while E-4031 is gradually blocking the HERG K^+ channel, Rb is gradually flowing out of the cell. The Rb outflow during this period will be added into the final Rb efflux total. This shifts the observed percentage inhibition toward the less potent direction. Therefore, a lower apparent potency is seen for E-4031 when compared with the potency obtained by electrophysiology. High extracellular K^+ concentration itself can also reduce the antagonist potency, as reported for E-4031 (37). This factor, combined with others discussed above, explains why Rb efflux results appear less potent than electrophysiology results.

So far, we have presented evidence to support the following conclusions. First, Rb efflux assay can be employed in HTS format to screen compounds against HERG K^+ channels. Second, it would be unrealistic to expect that the potency evaluation in Rb efflux assay will be as sensitive as the potency evaluation in electrophysiology, given the factors discussed above. The focus of the Rb efflux assay for HERG K^+ channels should be placed on the consistency and predictability of data generated. We ran the following experiments to address these issues. Close to 40 compounds were picked from our own chemical library and run in the Rb efflux assay for examination of their HERG activities. Table 1 shows the results of three independent Rb efflux assays done over a period of several months. Each assay result is expressed as mean and Standard Error of Mean (SEM) averaged from four wells. Consistent compound activities were observed, even though a slight variation from assay to assay was seen. This result, combined with the data discussed above (see Fig. 3A), shows that the assay is consistent and robust. Next we examined how predictable our Rb efflux assay was while using electrophysiology as the standard. Figure 7 shows percentage inhibition in electrophysiology assay vs. Rb efflux assay. For the electrophysiology assay, 3 μM concentration was used. Since we expected a reduction of apparent potency in Rb efflux assay (see data and discussion above), a higher concentration, 15 μM, was used in the Rb efflux assay. The averaged percentage inhibition and SEM (from three to five cells) in electrophysiology was plotted as the *X*-axis and the averaged percentage inhibition and SEM (from four wells) in Rb efflux assay was plotted as the *Y*-axis for a set of compounds, ranging from low to high HERG activity. The dashed line indicates the theoretical relationship between both assays if equal potency and Hill coefficient of 1 were assumed in both assays. For all 81 compounds, electrophysiology reveals a higher HERG inhibition than expected from the theoretical calculation based on Rb efflux result. This result is consistent with our above discussion that Rb efflux assay shifts the apparent potency to the less potent direction. If we use 30% inhibition as our cutoff threshold, 27 out of 81 compounds show more than 30% inhibition in Rb efflux assay. Of these 27 compounds, 26 also showed more than 30% inhibition in electrophysiology, even though a lower concentration (3 μM) was used in electrophysiology. There was only one compound that showed less than 30% (18.1%) inhibition in electrophysiology. However, when tested in a higher concentration (10 μM), the compound showed a strong blockade of HERG K^+ channels (data not shown). Based on this sample group, it appears that the Rb efflux assay could be relied upon to give positive predictions qualitatively for compounds antagonizing HERG K^+ channels. In a practical sense, if we use Rb efflux as a HERG activity filter for this sample group, 27 of 81 (33%) compounds could have been eliminated from electrophysiology assay. This significantly lowers the burden of electrophysiology assay. However, a compound that does not show HERG inhibition in this assay is not necessarily free of HERG activity. This point was exemplified by one of the test compounds indicated by the arrow in Fig. 7. In this case, the compound that showed close to 100% inhibition in electrophysiology at 3 μM concentration only registered a little over 20% inhibition in the Rb efflux, even though the test concentration (15 μM) was much higher in the efflux assay.

HTS functional assay for HERG K^+ channels is needed by pharmaceutical companies because of safety concerns for potential noncardiac drugs. Several forms of assays for HERG K^+ channels exist, including electrophysiology and dofetilide binding assays (18–20). Here we present another form of functional HERG assay that can be run as a HTS assay, i.e., 96-well/plate format. Under our testing conditions, a minimum of 700 compounds a day can be tested in a duplicate format by one person. At this rate, over 3000 compounds can be assayed within a week. With improvements in logistics and automation, significant increases could be achieved. The consistency of HTS assays is often as important as the throughput. Reliable assay results can be obtained as suggested in Fig. 3A and

Table 1

Results of Three Independent Rb Efflux Assays

	First Assay		Second Assay		Third Assay	
Compound #	% Inhibition	* SEM	% Inhibition	SEM	% Inhibition	SEM
1	0.3	0.5	−1.7	0.8	−2.4	0.4
2	3.4	0.7	0.7	0.6	5.0	3.3
3	14.4	1.4	6.6	0.5	7.3	0.5
4	47.4	1.1	44.4	0.9	42.8	4.0
5	39.8	3.2	28.4	2.4	26.4	1.7
6	0	0.5	−6.5	0.4	−3.9	0.8
7	0.9	0.7	−5.6	0.5	−3.8	2.0
8	2.8	1	−1.5	0.7	−0.4	1.2
9	2.4	1.2	−4.2	0.6	−2.1	0.5
10	17.7	1.4	10.3	2.4	14.9	1.6
11	19	2.7	14.1	2.4	14.5	0.9
12	30.2	1.7	26.1	3.8	22.3	2.6
13	4.2	0.4	1.3	0.8	3.7	1.3
14	−0.9	0.7	−1.9	2.3	−2.4	1.4
15	8	3	1.1	1.7	2.1	1.9
16	1.3	1.1	−2.7	1.2	−4.1	1.1
17	2.1	3.1	−1.9	2.2	−4.0	1.2
18	0.9	1	−1.7	2.6	−0.1	1.2
19	57.4	5.2	44.4	2	50.5	1.3
20	45.4	2.1	46.4	2.9	36.5	1.7
21	67.7	2.8	70.5	2.2	65.6	1.6
22	0.6	1	−1.8	0.9	2.0	1.1
23	−2.5	0.3	−1.7	1	1.3	1.8
24	47.9	1.3	56.3	2.1	65.9	2.0
25	15.4	2.2	12.7	2.3	12.6	2.2
26	36.1	0.9	30.9	1.7	36.2	1.2
27	19.4	1.3	12.8	1.9	18.3	2.0
28	−0.9	0.3	−1.8	0.9	−0.5	2.1
29	6.5	1.2	5.3	0.7	5.8	0.9
30	59.9	1	60.6	1.7	68.4	1.7
31	33.4	1.3	29.8	2.8	36.7	2.5
32	3.6	1.1	1	1	3.6	1.3
33	13.6	0.9	9.3	1.6	13.0	1.9
34	28.9	2.4	26.9	1.7	30.9	1.8
35	84.3	1.8	83.5	2.6	88.8	1.1
36	44.7	0.5	41.1	1.1	45.1	1.6
37	30.4	1.8	29.8	0.4	29.9	3.0

* SEM = Standard Error of Mean

Table 1. The reliability, high-throughput format, and nature of assaying functional activity of HERG K^+ channels make this assay highly desirable in the pharmaceutical industry.

Even though the Rb efflux assay is self-consistent, caution should be taken in the interpretation of the results, especially when comparing the results with data obtained through electrophysiology. Our data showed that evaluation of compound potency using Rb efflux depends on multiple factors, such as assay time, rate of Rb efflux, and kinetics of compound activity on HERG K^+ channels. Since

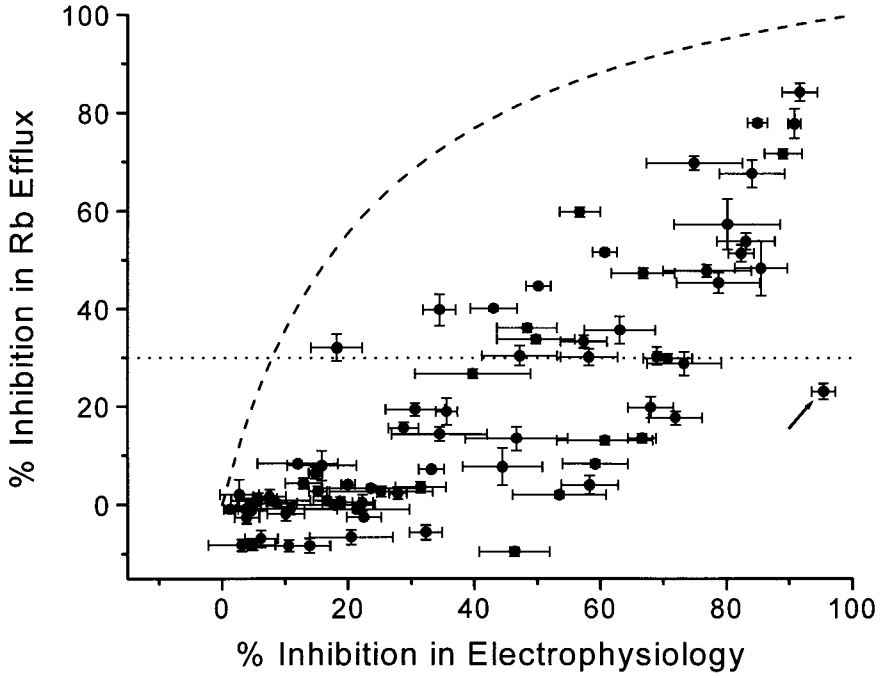

Figure 7. Comparison between Rb efflux and electrophysiology HERG assays. The *X*-axis represents percentage inhibition observed using a whole-cell voltage clamp at compound concentration of 3 μM. As in Fig. 6 for E-4031, the testing voltage was 3 mV for all compounds. Data represent the average recordings from three to five cells. The error bars represent SEM. The *Y*-axis represents percentage inhibition observed using Rb efflux assay at compound concentration of 15 μM. The assay was run at 30-min time point with 65 mM extracellular K^+ as stimulation. Ten micromoles of E-4031 was used as control and set as 100% blockade. The compound inhibition on HERG K^+ channels was normalized according to the E-4031 control. Data represent the average of four wells from one experiment in a 96-well/plate format. The error bars represent SEM. The dashed line indicates the theoretical relationship between both assays if equal potency and Hill coefficient of 1 are assumed. The dotted line indicates 30% inhibition in Rb efflux assay.

the amount of Rb efflux is collected at the end of the assay, the longer the assay time, the more Rb efflux will occur regardless of the blockage of a certain percentage of HERG K^+ channels. Therefore, it is not surprising to see that the compound potency was shifted toward the less potent direction when the assay time was extended. Furthermore, the extended assay time has a disproportionately larger impact on the apparent potency of weaker HERG antagonists than stronger ones. This effect should be reflected by the increase in Hill coefficient when the assay is run at a later time point. When we increased the assay time from 4 min to 40 min, the Hill coefficient was increased from 0.8 to 1.0 for E-4031, from 1.2 to 1.3 for NeurogenX, and from 1.0 to 1.2 for our model (see Fig. 5). Therefore, our results fit well with the theoretical principle of the Rb efflux through the HERG K^+ channel.

The Rb efflux rate, which can be affected by many factors, such as membrane potential or channel expression level on the cell membrane, can also affect the final evaluation of compound potency. As shown in Fig. 6A and B, a slower efflux rate can produce better estimates of compound potency. Even though many factors can be addressed theoretically and experimentally, controlling these factors in a HTS assay could prove problematic. For example, higher channel expression tends to produce higher efflux rate given all the other factors as equal. However, controlling the expression in a stable cell line is not facile and may not prove practical. Shortening the assay time improves the assay sensitivity, with the price being lower signal-to-noise ratio. Losses in the signal-to-noise ratio will hurt the overall quality of the data. Given the specific stable cell line we used, we recommended assaying

at ~30 min with 65 mM extracellular K^+ as stimulation, which provided the best signal-to-noise ratio.

The blocking kinetics of specific compounds on HERG K^+ channels, such as the slow blocking kinetics and nature of open channel blocker of E-4031 (see Fig. 6C), can also significantly alter the assay accuracy. Factors associated with specific compounds, such as fast vs. slow blocking and open channel antagonism vs. allosteric antagonism, can specifically affect the estimation of compound potency, though the effects of these factors cannot be generalized for the Rb efflux assay. Because different compounds may have different blocking kinetics on HERG K^+ channels, it is very difficult to deduce the electrophysiology IC_{50} value from the Rb efflux assay. If we consider the electrophysiology IC_{50} as the gold standard for evaluating the biophysical properties of a compound acting on HERG K^+ channels, it is clear that Rb efflux assay cannot provide the same overall sensitivity.

Even though there is a lack of one-to-one correlation of potency estimates between electrophysiology and Rb efflux assays, the Rb efflux assay can still provide useful insight into compound activity on HERG K^+ channels. As shown in our test samples (see Fig. 7), every compound that shows activity in Rb efflux (>30% inhibition) is confirmed to be active in electrophysiology, even though a lower concentration is used there. In other words, the Rb efflux assay is unlikely to give a false positive result for HERG activity. Therefore, we recommend using the Rb efflux assay as a HERG activity filter, through which a compound with potential cardiac side-effects could be removed from consideration for further development. As shown in Fig. 7, a significant portion of HERG active compounds could be eliminated by this filter, which could lower the burden of electrophysiology assay and speed up the compound development. Importantly, the high throughput format of the assay makes it possible to screen an entire chemical library, creating the ability to assess the level to which a library may be vulnerable to the liability of strong HERG activity.

ACKNOWLEDGMENTS

We would like to thank Drs. Jim Krause and Geoff White for their valuable comments and help in writing this manuscript.

REFERENCES

1. Warmke, J.W.; Ganetzky, B. Proc. Natl. Acad. Sci. USA **1994**, *91*, 3438–3442.
2. Curran, M.E.; Splawski, I.; Timothy, K.W.; Vincent, G.M.; Green, E.D.; Keating, M.T. Cell **1995**, *80*, 795–803.
3. Sanguinetti, M.C.; Jiang, C.; Curran, M.E.; Keating, M.T. Cell **1995**, *81*, 299–307.
4. Trudeau, M.C.; Warmke, J.W.; Ganetzky, B.; Robertson, G.A. Proc. Natl. Acad. Sci. USA **1995**, *269*, 92–95.
5. Roden, D.M.; Lazzara, R.; Rosen, M.; Schwartz, P.J.; Towbin, J.; Vincent, G.M. Circulation **1996**, *94*, 1996–2012.
6. Synders, D.J.; Chaudhary, A. Mol. Pharmacol. **1996**, *49*, 949–955.
7. Roy, M.; Dumaine, R.; Brown, A.M. Circulation **1996**, *94*, 817–823.
8. Rampe, D.; Roy, M.L.; Dennis, A.; Brown, A.M. FEBS Lett. **1997**, *417*, 28–32.
9. Suessbrich, H.; Waldegger, S.; Lang, F.; Busch, A.E. FEBS Lett. **1996**, *385*, 77–80.
10. Ben-Davis, J.; Zipes, D.P. Lancet **1993**, *341*, 1578–1582.
11. Pourrias, B.; Porsolt, R.D.; Lacroix, P. Drug Dev. Res. **1999**, *47*, 55–62.
12. Crumb, W.; Cavero, I. PSTT **1999**, *2*, 270–280.
13. CPMP. Points to Consider: The Assessment of the Potential for QT Interval Prolongation by Non-cardiovascular Medicinal Products. Committee for Proprietary Medicinal Products (CPMP), Human Medicines Evaluation Unit, Publication No. CPMP 986 96, 1997.
14. Li, G.-R.; Feng, J.; Yue, L.; Carrier, M.; Nattel, S. Circ. Res. **1996**, *78*, 689–696.
15. Johnson, J.P.; Mullins, F.M.; Bennet, P.B. J. Gen. Physiol. **1999**, *113*, 565–580.
16. Smith, P.L.; Baukrowitz, T.; Yellen, G. Nature **1996**, *379*, 833–836.
17. Kiehn, J.; Lacerda, A.E.; Wible, B.; Brown, A.M. Circulation **1996**, *94*, 2572–2579.
18. Michne, W.F.; Guiles, J.W.; Treasurywala, A.M.; Castonguay, L.A.; Weigelt, C.A.; Oconnor, B.; Volberg, W.A.; Grant, A.M.; Chadwick, C.C.; Krafte, D.S.; Hill, R.J. J. Med. Chem. **1995**, *38*, 1877–1883.
19. Chadwich, C.C.; Ezrin, A.M.; Oconner, B.; Volberg, W.A.; Smith, D.I.; Wedge, K.J.; Hill, R.J.; Briggs, G.M.; Pagani, E.D.; Silver, P.J.; Kraffe, D.S. Circ. Res. **1993**, *72*, 707–714.
20. Lynch, J.J.; Baskin, E.P.; Nutt, E.M.; Guinosso, P.J.; Hamill, T.; Salata, J.J.; Woods, C.M. J. Card. Pharmacol. **1995**, *25*, 336–340.
21. Finlayson, K.; Pennington, A.J.; Kelly, J.S. Eur. J. Pharmacol. **2001**, *412*, 203–212.

22. De Silva, H.A.; Aronson, J.K.; Grahame-Smith, D.G.; Jobst, K.A.; Smith, A.D. Lancet **1998**, *352*, 1590–1593.
23. Linde, C.; Loffler, C.; Kessler, C.; Quast, U. Naunyn Schmiedebergs Arch. Pharmacol. **1997**, *356*, 467–474.
24. Miller, S.S.; Edelman, J.L. J. Physiol. (Lond.) **1990**, *424*, 283–300.
25. Castelletti, L.; Memo, M.; Missale, C.; Spano, P.F.; Valerio, A. J. Physiol. (Lond.) **1989**, *410*, 251–265.
26. Jacques, Y.; Romey, G.; Lazdunski, M. Eur. J. Biochem. **1980**, *111*, 265–273.
27. Palfrey, C.; Littauer, U.Z. Biochem. Biophys. Res. Commun. **1976**, *72*, 209–215.
28. Frelin, C.; Vigne, P.; Lazdunski, M. Eur. J. Biochem. **1981**, *119*, 437–442.
29. Hamill, O.P.; Marty, A.; Neher, E.; Sakmann, B.; Sigworth, F.J. Pflugers Arch. **1981**, *391*, 85–100.
30. Walker, B.D.; Valenzuela, S.M.; Singleton, C.B.; Tie, H.; Bursill, J.A.; Wyes, K.R.; Qiu, M.R.; Breit, S.N.; Campbell, T.J. Br. J. Pharmacol. **1999**, *127*, 243–251.
31. Zhou, Z.; Gong, Q.; Ye, B.; Fan, Z.; Makielski, J.C.; Robertson, G.A.; January, C.T. Biophys. J. **1998**, *74*, 230–241.
32. Spector, P.S.; Curran, M.E.; Keating, M.T.; Sanguinetti, M.C. Circ. Res. **1996**, *78*, 499–503.
33. Abbott, G.W.; Sesti, F.; Splawski, I.; Buck, M.E.; Lehmann, M.H.; Timothy, K.W.; Keating, M.T.; Goldstein, S.A.N. Cell **1999**, *97*, 175–187.
34. Ficker, E.; Jarolimek, W.; Kiehn, J.; Baumann, A.; Brown, A.M. Circ. Res. **1998**, *82*, 386–395.
35. Zhou, Z.; Vorperian, V.R.; Gong, Q.; Zhang, S.; January, C.T. J. Card. Electrophysiol. **1999**, *10*, 836–843.
36. Sanguinetti, M.C.; Jurkiewicz, N.K. Pflugers Arch. **1992**, *420*, 180–186.
37. Wang, S.; Morales, M.J.; Liu, S.; Strauss, H.C.; Rasmusson, R.L. FEBS Lett. **1997**, *417*, 43–47.